Science of the Total Environment 797 (2021) 149034

Contents lists available at ScienceDirect

Science of the Total Environment

journal homepage: www.elsevier.com/locate/scitotenv

Accuracy assessment of remotely sensed data to analyze lake water balance in semi-arid region

Joy Bhattacharjee [a,*], Mehedi Rabbil [a], Nasim Fazel [a,b], Hamid Darabi [a], Bahram Choubin [c], Md. Motiur Rahman Khan [a], Hannu Marttila [a], Ali Torabi Haghighi [a]

[a] Water, Energy and Environmental Engineering Research Unit, PO Box 4300, FI-90014, University of Oulu, Finland
[b] Freshwater Centre, Finnish Environment Institute (SYKE), Helsinki, Finland
[c] Soil Conservation and Watershed Management Research Department, West Azarbaijan Agricultural and Natural Resources Research and Education Center, AREEO, Urmia, Iran

HIGHLIGHTS

- Water balance algorithms were used to simulate semi-arid lake water levels.
- Scenarios were formed by combining in-situ and remote sensing data sources.
- The proposed combinations can reproduce lake water level even without in-situ data.
- Using in-situ data as initial water level matched best to simulate lake water level.
- 9 out of 19 scenarios did not vary significantly with in-situ water level.

GRAPHICAL ABSTRACT

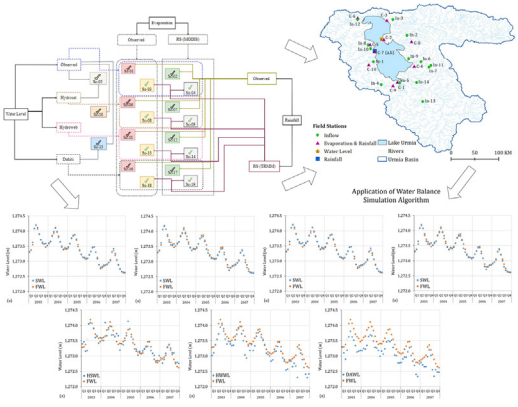

ARTICLE INFO

Article history:
Received 29 March 2021
Received in revised form 28 June 2021
Accepted 9 July 2021
Available online 14 July 2021

Editor: Ouyang Wei

Keywords:
Inland water
Scenario
Water management
Meteorological data

ABSTRACT

Lake water level fluctuation is a function of hydro-meteorological components, namely input, and output to the system. The combination of these components from in-situ and remote sensing sources has been used in this study to define multiple scenarios, which are the major explanatory pathways to assess lake water levels. The goal is to analyze each scenario through the application of the water balance equation to simulate lake water levels. The largest lake in Iran, Lake Urmia, has been selected in this study as it needs a great deal of attention in terms of water management issues. We ran a monthly water balance simulation of nineteen scenarios for Lake Urmia from 2003 to 2007 by applying different combinations of data, including observed and remotely sensed water level, flow, evaporation, and rainfall. We used readily available water level data from Hydrosat, Hydroweb, and DAHITI platforms; evapotranspiration from MODIS and rainfall from TRMM. The analysis suggests that the consideration of field data in the algorithm as the initial water level can reproduce the fluctuation of Lake Urmia water level in the best way. The scenario that combines in-situ meteorological components is the closest match to the observed water level of Lake Urmia. Almost all scenarios showed good dynamics with the field water level, but we found that nine out of nineteen scenarios did not vary significantly in terms of dynamics. The results also reveal that, even without any field data, the proposed scenario, which consists entirely of remote sensing components, is capable of estimating water level fluctuation in a lake. The analysis also explains the necessity of using proper data sources to act on water regulations and managerial decisions to understand the temporal phenomenon not only for Lake Urmia but also for other lakes in semi-arid regions.

* Corresponding author at: Water, Energy and Environmental Engineering Research Unit, PO Box 4300, 90014, University of Oulu, Finland.
E-mail address: joy.bhattacharjee@oulu.fi (J. Bhattacharjee).

https://doi.org/10.1016/j.scitotenv.2021.149034

1. Introduction

Every physical and ecological process in lakes is strongly linked to water level fluctuation (WLF) (Leira and Cantonati, 2008). Accurate estimation and predictions of possible changes in WLF, due to hydro-meteorological variations and anthropogenic disturbances, are essential for proper water resources management in the lake basin (Hofmann et al., 2008), particularly in water-limited (i.e., arid and semi-arid) regions (Jafari et al., 2019). The WLF in a lake is a result of complex interactions including hydrological process (fluctuations in surface and groundwater), meteorological components, pressure change condition over the lake surface, circulation processes, and wind events, whereas water balance (WB) is more affected by meteorological components, and inflow-outflow volumes (Schmied et al., 2016; Torabi Haghighi and Kløve, 2015).

Due to a lack of reliable field measurements of meteorological and hydrological components, lake water level (WL) assessment has become challenging and costly in many cases (Torabi Haghighi et al., 2018). Many lakes in remote locations are not well monitored because of limited human and economic resources (Fazel et al., 2017; Medina et al., 2008). Satellite-derived hydro-meteorological measurements have created greater opportunities through the application of remotely sensed components in water resources management (Anagnostou, 2004), although the variability of these sources contains spatiotemporal limitations in different regions.

Investigating WL dynamics, satellite altimetry (Buma and Lee, 2016; Crétaux et al., 2011; Medina et al., 2008; Zhang et al., 2011) and integrating meteorological data into hydrological models; satellite missions, such as TRMM (Tropical Rainfall Measuring Mission), TMPA (TRMM Multi-satellite Precipitation Analysis) and MODIS (Moderate Resolution Imaging Spectroradiometer) has become popular (Akbari et al., 2019). These resources can also be used to analyze lake water surface-volume relations, to assess water flow alteration (Akbari et al., 2020; Rokni et al., 2014), and to monitor open water surface (Torabi Haghighi et al., 2016). However, the application of remotely sensed hydro-meteorological components still needs further assessment, compared with the combination of in situ and satellite data to estimate WLF (Jafari et al., 2019).

At present, several open-source platforms provide lake WL based on space-borne geodetic sensors (Schwatke et al., 2015). The accuracy of estimated WL in comparison with observed field measurements varies and depends on the availability of the mission's coverage and the location of the desired lake. Thus, the accuracy of estimating WL through geodetic sensors still needs to be investigated for each case individually. It also raises the question of how analysis of lake WB can be realistic when the simulation of lake WB is based on different sources, including remote sensing (RS) and in-situ data. Furthermore, it is important to know what combination techniques of in-situ and RS data are optimum for WB analysis and to address the influence of each component of WB on the lake's WLF.

In this study, we used the lake water balance equation to investigate the applicability and efficiency of field and satellite measurements to simulate lake WL. The combination of different hydro-meteorological components from multiple sources was used to define various scenarios, and to simulate lake WL. Furthermore, the proposed framework was tested in Lake Urmia, the largest Iranian inland water body, in different scenarios for the period 2003–2007.

2. Materials and methods

To estimate lake WL, we proposed a scenario-based WB simulation framework. The framework provides the simulated WL of Lake Urmia by analyzing WB based on the available meteorological and hydrological components or the lake's altimetry for 19 different combinations of available in-situ and RS data (Fig. 1). The accuracy of simulated WL in each scenario was assessed based on the available observed WL. To apply our algorithm, Lake Urmia in Iran was selected as a case study. The complete process of simulating WL using remotely sensed products and applying them to Lake Urmia for different proposed scenarios includes scenario generation using the available data sources and analysis through the WB simulation algorithm (Fig. 1).

2.1. Study area

Lake Urmia is the largest inland water body (maximum 6000 km^2 area), located in the northwest of Iran (Fig. 2a). The lake is listed as a biosphere reserve by UNESCO and was listed as a Ramsar site in 1995 (Barhagh et al., 2021; Rezaei Zaman et al., 2016). The lake is a terminal lake and supports vast biodiversity in the region (Sima et al., 2021). Cropland and orchards cover 10% of the basin area (52,000 km^2) but consume more than 90% of all renewable water resources in the basin (Fazel et al., 2017). The major source of water demand related to agriculture originates from surface water. The natural flow of surrounding rivers in Lake Urmia basin was affected by the construction of large dams along the main watercourses (Torabi Haghighi et al., 2018). The precipitation in the basin occurs mainly in winter and spring. During 1965–2010 the mean annual precipitation was around 357 mm whereas the annual potential evaporation varied from 1050 mm to 1550 mm from the northeast to the southwest (Fazel et al., 2017). Djamali et al. (2008) also reported 11.2 °C mean annual temperature during 1951–2010 in Lake Urmia. More than 75% of lake inflow is supplied by surrounding main rivers as listed in Fig. 2b. There are surface water monitoring stations available on the main rivers which are denoted as In-1 to In-14 in Fig. 2.

2.2. Data collection and preliminary assessment

To process WL simulation, we used available RS data from different sources and field measurements from nearby stations around Lake Urmia (see Table A.1 in Supplemental Materials (SM)-A for detailed information of collected data).

2.2.1. Water level (WL)

We collected four readily available WL time series of Lake Urmia from 2001 to 2013. The collected WL data includes field measurements at Lake Urmia (F_{WL}), estimated measurements from Hydrosat (HS_{WL}), Hydroweb (HW_{WL}), and DAHITI (DA_{WL}) databases. Daily field WL measurements were collected by corresponding officials from the limnimeter which was installed on the pillar of Lake Urmia bridge (yellow color pentagon in Fig. 2a).

To monitor the global water cycle, the Institute of Geodesy (GIS) at the University of Stuttgart developed the Hydrosat platform where they used space-borne geodetic sensors to estimate WL (Hydrosat, 2021). Hydroweb, another platform of RS WL, was also used in this study. It covers a multi-satellite mission to estimate lake WL as mentioned by Crétaux et al. (2011) (Hydroweb, 2021). Schwatke et al. (2015) used another database, DAHITI, to monitor the hydrological time series of inland water bodies in their studies; based on multi-mission satellite altimetry. The German Geodetic Research Institute, DGFI-TUM (DAHITI, 2021), developed this platform in 2013, providing an extended high temporal resolution dataset with 10-day to 35-day time intervals from 1992.

2.2.2. Flow data

The daily flow data was used to calculate the total inflow to the lake. For this purpose, we collected flow data from 14 gauges on the main rivers around the lake. Some of the In-y gauge stations (y refers to numbers from 1 to 14 in Fig. 2) were not very close to Lake Urmia but for each river, the selected gauge was the closest flow measurement point to the lake (Fig. 2). All data was acquired from the Iranian water resource management authorities. Fig. 2b represents the available period of inflow data from these surrounding rivers. Based on the temporal availability of flow and meteorological data, we looked at five years from 2003 to 2007 in this study to apply the proposed scenario to simulate the WL of Lake Urmia.

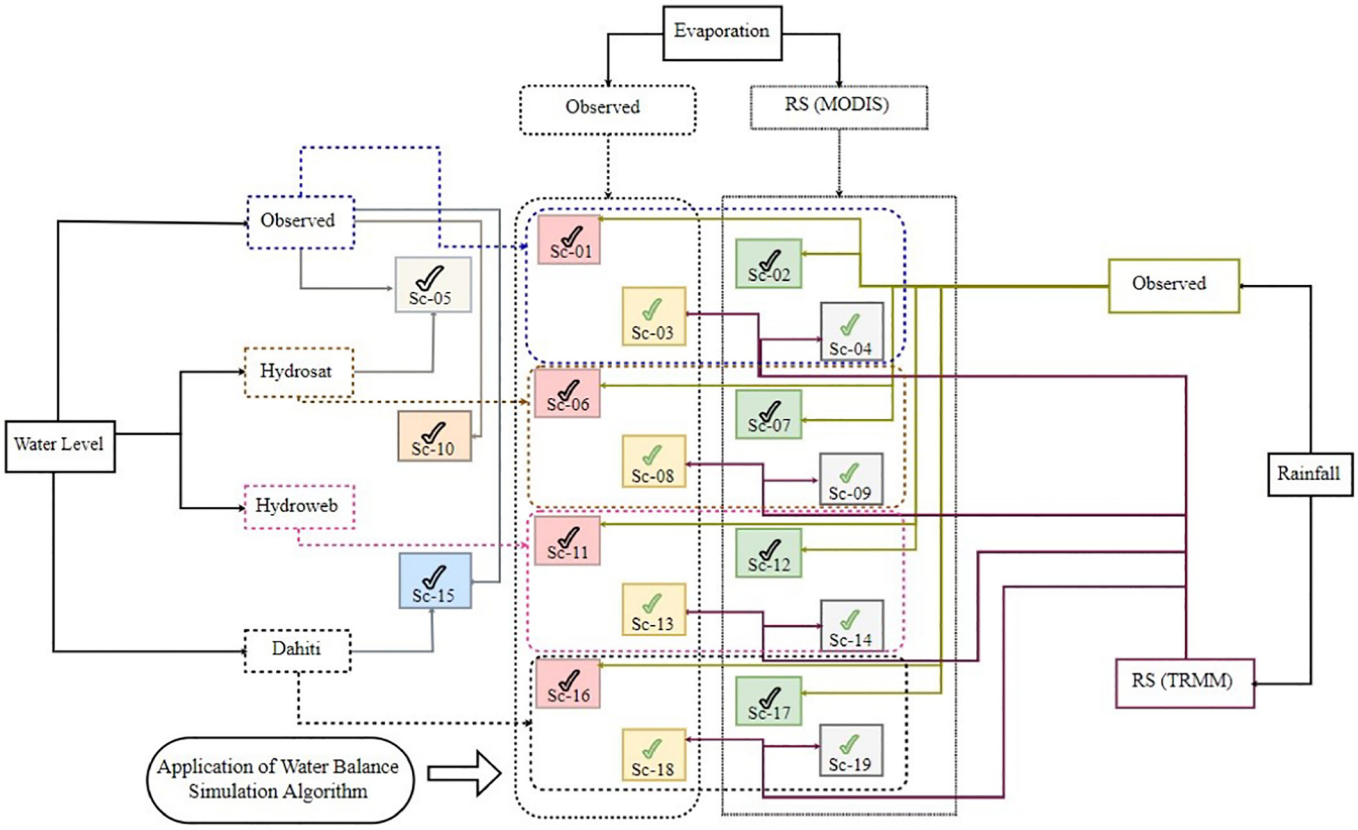

Fig. 1. Detailed component of each scenario formation to apply WB simulation algorithm. For example, Sc-01 simulates WL based on the provided data source of observed WL, observed evaporation, and observed rainfall.

2.2.3. Evaporation, evapotranspiration, and rainfall data sources

Two major variables in lake water balance simulation are evaporation and rainfall. As Lake Urmia is a closed lake, evaporation is responsible for the main outflow of the lake. Eleven meteorological stations, including Dashkhaneh (C-1), Islamic-Island (C-2), Sharafkhaneh (C-3), Bonab (C-4), Abajalusofla (C-5), Yalquzchy (C-6), Azarshar (C-8), Mehmandar (C-9), and Ghasemloo (C-10), were used to collect daily field evaporation and rainfall data (purple color triangles in Fig. 2a). For station C-7 at Tabgolshi, there were two measurement stations known as Tabgolshi Freshwater station (FWS) (C-7a) and Tabgolshi Salty water station (SWS) (C-7b).

During 2003–2007, each evaporation and rainfall station had different dynamics. Therefore, in the lake WB simulation process, instead of using evaporation and rainfall for each station at a time, we used spatially interpolated values of field evaporation and rainfall data (Fig. B.1 in SM-B). We used the Kriging method for the basin area as mentioned by Taheri et al. (2018) based on all available stations provided in Fig. 2a. To use spatially interpolated values only for the lake, first, we estimated the boundary of Lake Urmia during 2003–2007 based on the NDWI measurements from the climate engine platform (Huntington et al., 2017). Then, we extracted the interpolated pixel value within the boundary. Therefore, the evaporation rate in Fig. B.1 in SM-B represents the amount of evaporated water inside the lake wet area.

We collected MODIS evapotranspiration (ET) data from the climate engine platform. RS values were consistent with field evaporation data throughout the analysis period from 2003 to 2007. Table C.1 in SM-C showed a good correlation between the field data of each station and remote sensing ET, with Bonab and Abajalusofla stations showing the highest correlation (0.96, $p > 0.05$) with RS data. Even observed evaporation stations from C1 to C10 showed a good correlation (R^2 ~ above 0.85) with each other when averaged by month.

For RS precipitation, gridded TRMM RS data with 3-hour temporal resolution and a 0.25-degree spatial resolution were collected. The consistency was also noticeable between field rainfall and RS rainfall (Fig. D.1 in SM-D). RS rainfall showed no significant difference ($R^2 = 0.92$, p-value (0.1431) > 0.05) with field rainfall, although we found overestimated RS data for some months, especially during high and low peaks.

2.3. Scenario generation

We combined RS data and field measurements to produce 19 scenarios (Sc-01-Sc-19 in Table 1 and Fig. 1). To generate these scenarios, we considered the combination of different sources of WL, rainfall, field evaporation, and RS ET. Lake inflow (integrated monthly flows of 14-gauge stations) was the same in all scenarios, due to RS flow data being unavailable. We divided all the scenarios into four different groups based on the initial WL (HS_{WL} or HW_{WL} or DA_{WL}) used in the simulation (Table 1, column 2).

Out of 19 scenarios, the first scenario (Sc-01) was developed entirely based on the observed field data, whereas for Sc-09, Sc-14, and Sc-19 we considered RS input data for all components. The rest of the scenarios were generated based on a combination of field and RS data (Table 1).

The output of each scenario was simulated WL (S_{WL}) to be compared with field WL (F_{WL}) (Table 1, column 6) for the assessment of the best scenario. For Sc-05, Sc-10, and Sc-15, readily available WL data (HS_{WL}, HW_{WL}, and DA_{WL}) was collected from different platforms (DAHITI, 2021; Hydrosat, 2021; Hydroweb, 2021) and was directly compared with F_{WL}.

2.4. Application of the WB simulation algorithm

The monthly lake WL was simulated as a function of hydro-climatological components of water balance (Eq. (1)) for all scenarios, except Sc-05, Sc-10, and Sc-15.

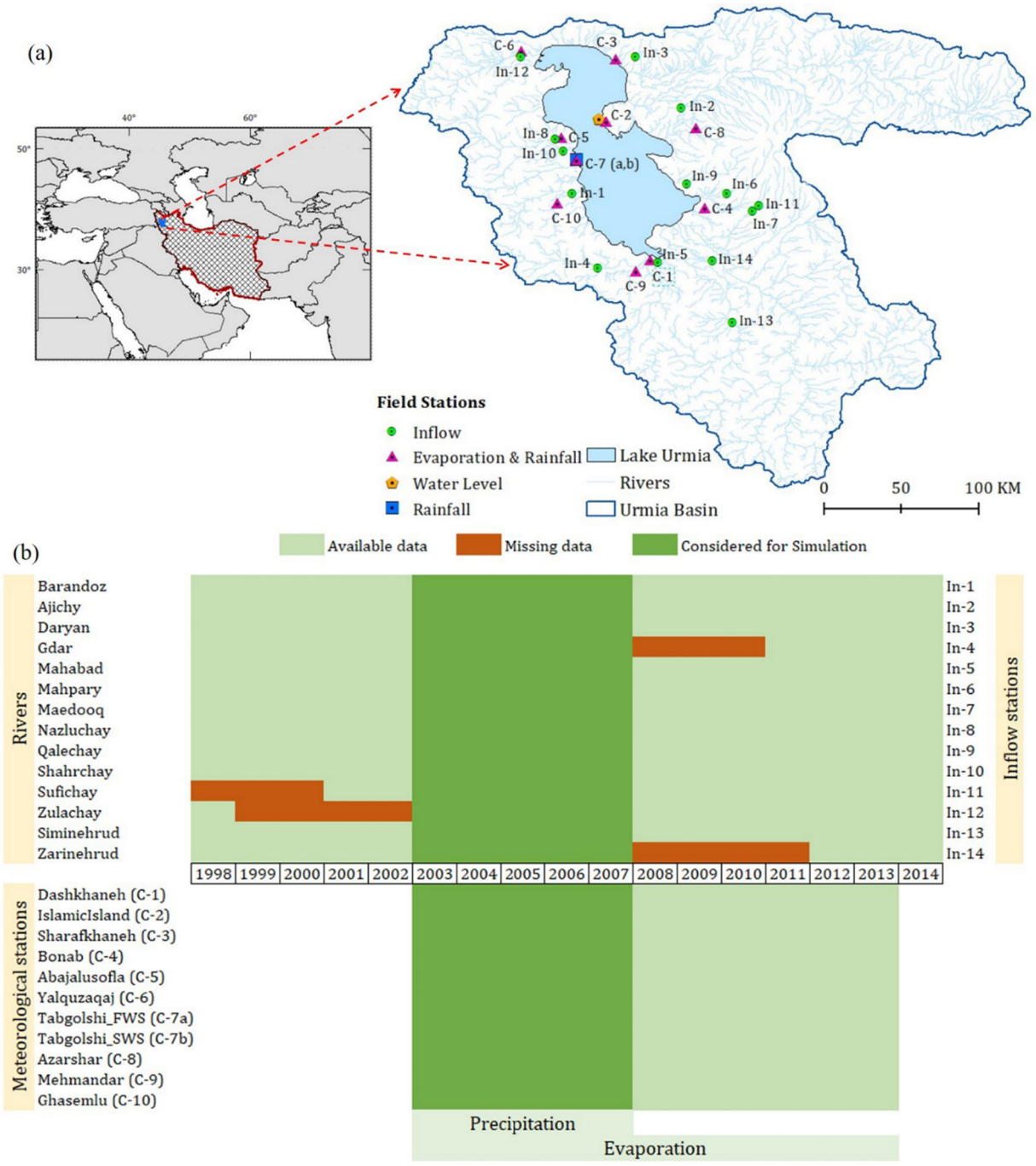

Fig. 2. Study area and layout of in-situ data: (a) Lake Urmia with available nearby hydro-climatology and WL observation stations where all climate stations are labeled as C-x (x refers to numbers from 1 to 10, for number 7 there are two stations for fresh water and salty water). All inflow stations for contributing rivers are labeled as In-y (y refers to numbers from 1 to 14) with (b) available period of flow data at the outlet of main rivers in Lake Urmia basin and available meteorological data (bottom part of b), where the green color represents considered simulation period based on data availability of all corresponding monitoring stations. (For interpretation of the references to color in this figure legend, the reader is referred to the web version of this article.)

$$Lake\ water\ level = f(inflow, evaporation, rainfall, groundwater\ flux) \quad (1)$$

We used a MATLAB script developed by Torabi Haghighi et al. (2018) for Lake Urmia to simulate lake WL. Based on the following equation, the script considered monthly time step due to the resolution of RS WL and ET data (all in-situ data was available in the daily time scale):

$$V_{i+1} = V_i\ (\text{Storage}) + (\text{inflow}(\sum Q_I) - \text{outflow}(\sum Q_o))_i \quad (2)$$

The equation (Eq. (2)) calculates the volume of stored water at the onset of the month ahead (V_{i+1}) based on the water storage at the beginning of the current month (V_i) and the amount of inflow and outflow over the current month.

$$\text{Inflow}(\sum Q_I) = R_I + P_I \quad (3)$$

$$\text{Outflow}(\sum Q_o) = E_o \quad (4)$$

where P is rainfall and R is an inflow to the lake from surrounding rivers; these are considered as a total inflow (Eq. (3)). As evaporation is the only source of outflow (Eq. (4)) from the lake; for scenarios (Sc-01, Sc-03, Sc-06, Sc-08, Sc-11, Sc-13, Sc-16, and Sc-18) we used observed potential evaporation from the pan and we applied pan coefficient (c

Table 1
Designed scenarios with a combination of available field and RS data.

Group	Scenario	Initial WL	Precipitation (P)	E or ET	EBCB[1]
I	Sc-01	Field	Field	Field	F_{WL} & S_{WL}
	Sc-02	Field	Field	RS	F_{WL} & S_{WL}
	Sc-03	Field	RS	Field	F_{WL} & S_{WL}
	Sc-04	Field	RS	RS	F_{WL} & S_{WL}
II	Sc-05	Hydrosat	–	–	F_{WL} & HS_{WL}
	Sc-06	Hydrosat	Field	Field	F_{WL} & S_{WL}
	Sc-07	Hydrosat	Field	RS	F_{WL} & S_{WL}
	Sc-08	Hydrosat	RS	Field	F_{WL} & S_{WL}
	Sc-09	Hydrosat	RS	RS	F_{WL} & S_{WL}
III	Sc-10	Hydroweb	–	–	F_{WL} & HW_{WL}
	Sc-11	Hydroweb	Field	Field	F_{WL} & S_{WL}
	Sc-12	Hydroweb	Field	RS	F_{WL} & S_{WL}
	Sc-13	Hydroweb	RS	Field	F_{WL} & S_{WL}
	Sc-14	Hydroweb	RS	RS	F_{WL} & S_{WL}
IV	Sc-15	DAHITI	–	–	F_{WL} & DA_{WL}
	Sc-16	DAHITI	Field	Field	F_{WL} & S_{WL}
	Sc-17	DAHITI	Field	RS	F_{WL} & S_{WL}
	Sc-18	DAHITI	RS	Field	F_{WL} & S_{WL}
	Sc-19	DAHITI	RS	RS	F_{WL} & S_{WL}

[1] EBCB: Evaluation based on the comparison between, F_{WL} (Field WL) and S_{WL} (Simulated WL). HS_{WL}, HW_{WL}, DA_{WL}: Estimated WL from Hydrosat, Hydroweb, and DAHITI dataset.

as evaporation coefficient (~0.7) (Torabi Haghighi and Kløve, 2015) to estimate actual evaporation (E_o) of the lake. For remote sensing ET, we considered E_o as being the same as collected values from MODIS. After integrating all components, we used the following equation as the final WB equation to simulate lake WL:

$$V_{i+1} = V_i(\text{Storage}) + R_{Ii} + (10e^{-6}(P - (E_o) * A)_i \quad (5)$$

where V_{i+1} and V_i are the volume of the lake (km^3) at the start of the current and following month, R_I is the volume of inflow to the lake in the current months (km^3), P is the amount of rainfall to the lake (mm), E_o is the amount of actual evaporation from the lake surface (mm), and A is the mean area of the lake in the current month (km^2). Next, to estimate WL and area from the calculated volume in each scenario (except scenarios Sc-05, Sc-10, and Sc-15), we:

- acquired initial WL for the onset of each month from a relevant source (column 2, Table A.1).
- converted the acquired WL to volume based on the area volume depth relationship developed by Sima and Tajrishy (2013) for Lake Urmia.
- considered hydro-meteorological components and calculated the volume of the lake at the end of the month, and
- converted the calculated volume to WL using the area volume depth relationship.

In WB simulation, groundwater flux and the contribution of mid-basin (between flow measuring points (gauges location) and the points where the water discharged to the lake) were not considered.

2.5. Evaluation of scenarios

After estimating WL using the WB simulation algorithm, we tested the goodness of fit of each scenario between S_{WL} and F_{WL} using the non-parametric Mann-Whitney *U* test with a 0.05 significance level. For each year, we hypothesized that the median of S_{WL} was equal to the median of F_{WL}. To understand how our assumption resulted in the simulated lake WL:

- we used a scatterplot to focus on the variations
- the correlation coefficient was considered as a statistical measurement to define the relationship strength between two WL time series

Deviations estimated from F_{WL} were also considered to assess each scenario through the root mean square error (RMSE) and the sum of the squared estimate of errors (SSE).

3. Results

3.1. Sc-01 to Sc-04: using F_{WL} as initial WL to simulate lake WL

Consideration of F_{WL} as initial WL showed a mean difference of 0.02 m between F_{WL} and S_{WL} for scenarios Sc-01 to Sc-04. During 2003–2007, we noticed underestimated S_{WL} as compared to F_{WL} for all years except for 2003. The difference varied from 0.01 m to 0.04 m on average for Sc-01 (WL, P, and E in the field) and Sc-02 (WL, P in the field, and RS ET). When RS precipitation was used in Sc-03 (WL and E in the field) and Sc-04 (WL in the field and RS ET), we found S_{WL} variations from 0.01 m to 0.03 m on average (Fig. 3). The trend of both water levels followed each other. For all four scenarios, the association between F_{WL} and S_{WL} was around 0.99 representing a strong relationship (p-value >0.05).

3.2. Sc-06 to Sc-09: using HS_{WL} as initial WL to simulate lake WL

The difference between S_{WL} and F_{WL} fluctuated from 0.4 m to 0.5 m for scenarios Sc-06 to Sc-09 for Lake Urmia as the S_{WL} was slightly overestimated, especially during 2003–2005 (Fig. 4). In July 2003, the difference was highest, varying from 0.41 m to 0.47 m. This difference was also visible in Fig. 4c, where it showed increased scattered behavior especially when F_{WL} was higher than 1273.9 m but less than 1274.2 m. After 2005, S_{WL} showed a better pattern with F_{WL}, where we found a 0.1 m average difference (correlation coefficient ~ 0.86 on average for p-value >0.05).

3.3. Sc-11 to Sc-14: using HW_{WL} as initial WL to simulate lake WL

We noticed underestimated S_{WL} concerning F_{WL} from Sc-11 to Sc-14 while considering HW_{WL} as the initial WL. The Mann-Whitney *U* test also resulted in significant differences (p-value <0.05) between S_{WL} and F_{WL}, although the dynamics were highly correlated (correlation coefficient ~ 0.87). The difference varied from 0.06 m to around 1 m on average for all four scenarios (Fig. 5).

3.4. Sc-16 to Sc-19: using DA_{WL} as initial WL to simulate lake WL

The dynamics of S_{WL} were better when we considered the DAHITI database as initial WL from Sc-16 to Sc-19, although S_{WL} deviated from F_{WL} with an almost constant difference for each year. The simulated WL differed from 0.03 m to 0.6 m on average for all four scenarios (Fig. 6). Therefore, significant differences (p-value <0.05) were found from the Mann-Whitney U test between the simulated and field WL.

3.5. S_{WL} based on estimated readily available WL from spaceborne geodetic sensors

The collected readily available WL data from the Hydrosat platform did not show significant differences (p-value >0.05) with the observed WL data from Lake Urmia. Hydrosat WL showed a comparatively closer agreement with F_{WL} concerning the other two sensor-based WL time series. During 2003–2007, Hydrosat WL in Sc-05 was 0.11 m higher than F_{WL} on average (Fig. 7).

The median of observed WL data varied significantly (p-value <0.05) with the WL database from Hydroweb and DAHITI. For Hydroweb, the observed WL was 0.2 m higher (on average) in 2003 and the situation was the same for HW_{WL} throughout the period. The estimated WL from DAHITI was almost the same as the observed data at the beginning of 2003. For the entire period, WL from DAHITI showed substantial underestimation from F_{WL}, although we found better dynamics concerning all other readily available WL time series (Fig. 7).

4. Discussion

For nine out of the nineteen scenarios, we found the simulated water levels did not show significant differences with the field water level data

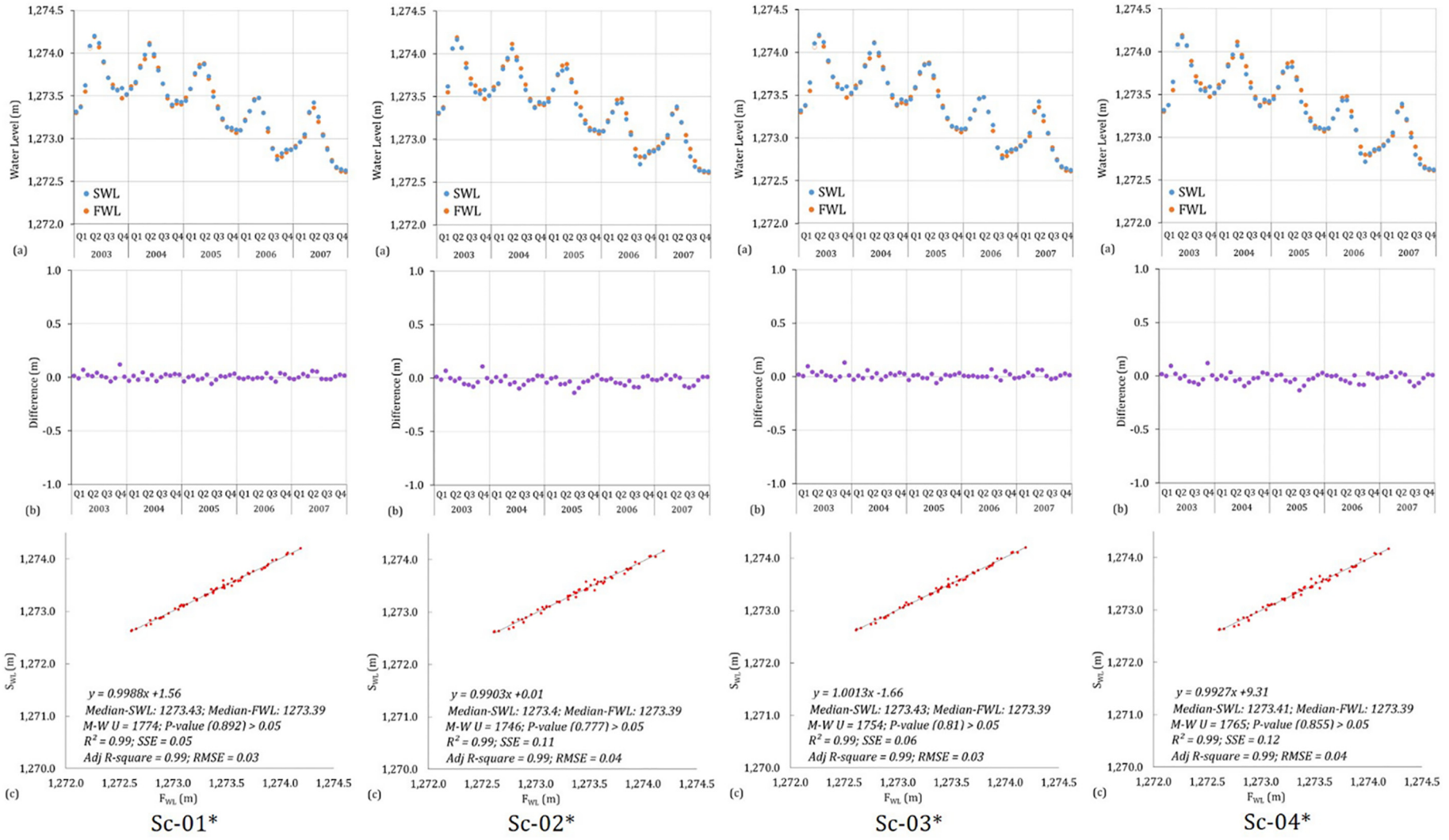

Fig. 3. Combination of different data sources based on F_{WL} as initial WL of the simulation to simulate WL in Lake Urmia for Sc-01 to Sc-04.* indicates no significant differences between S_{WL} and F_{WL}.

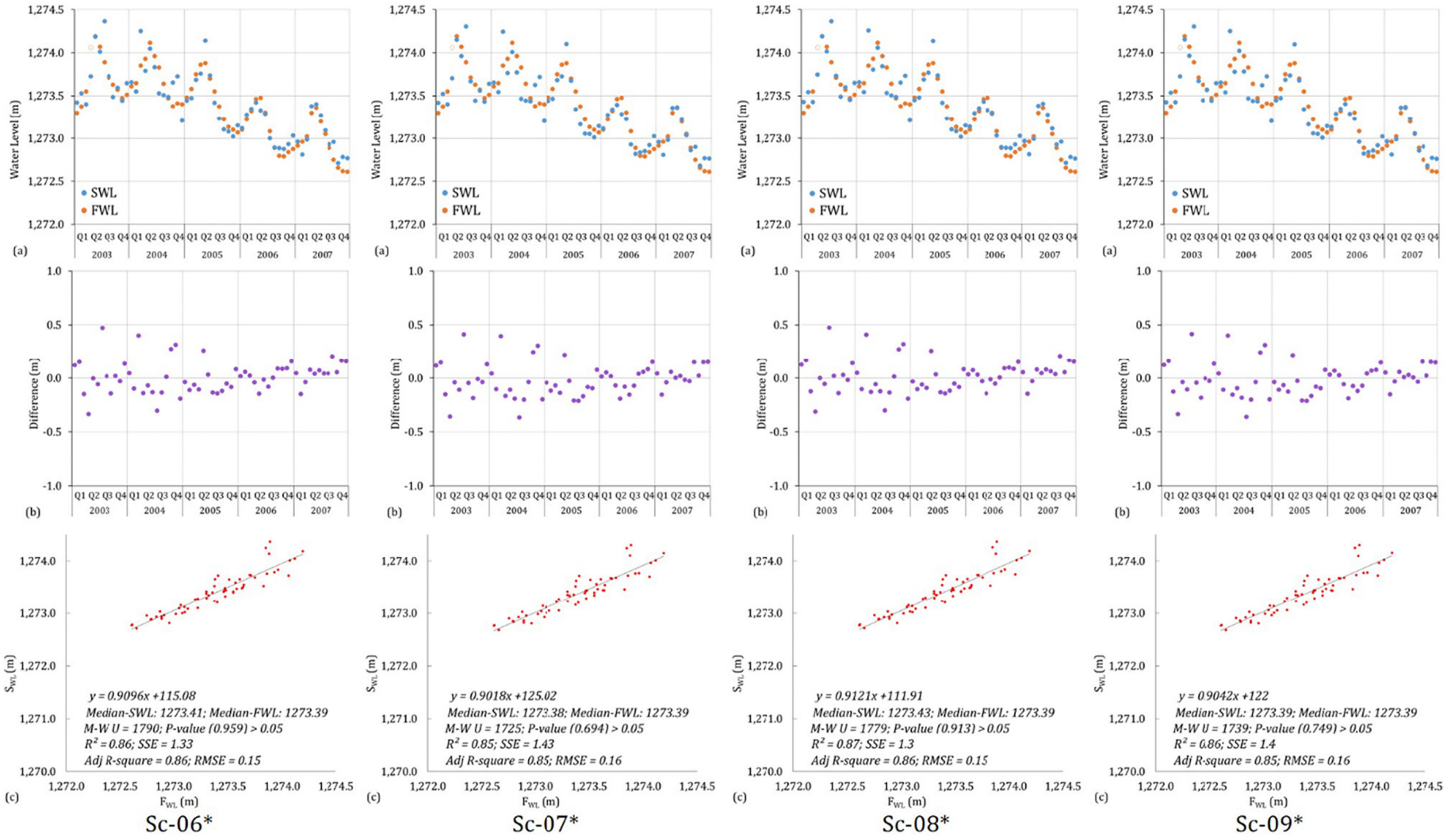

Fig. 4. Combination of different data sources considering HS_{WL} as initial WL of the simulation to simulate WL in Lake Urmia for Sc-06 to Sc-09. * indicates no significant differences between S_{WL} and F_{WL}.

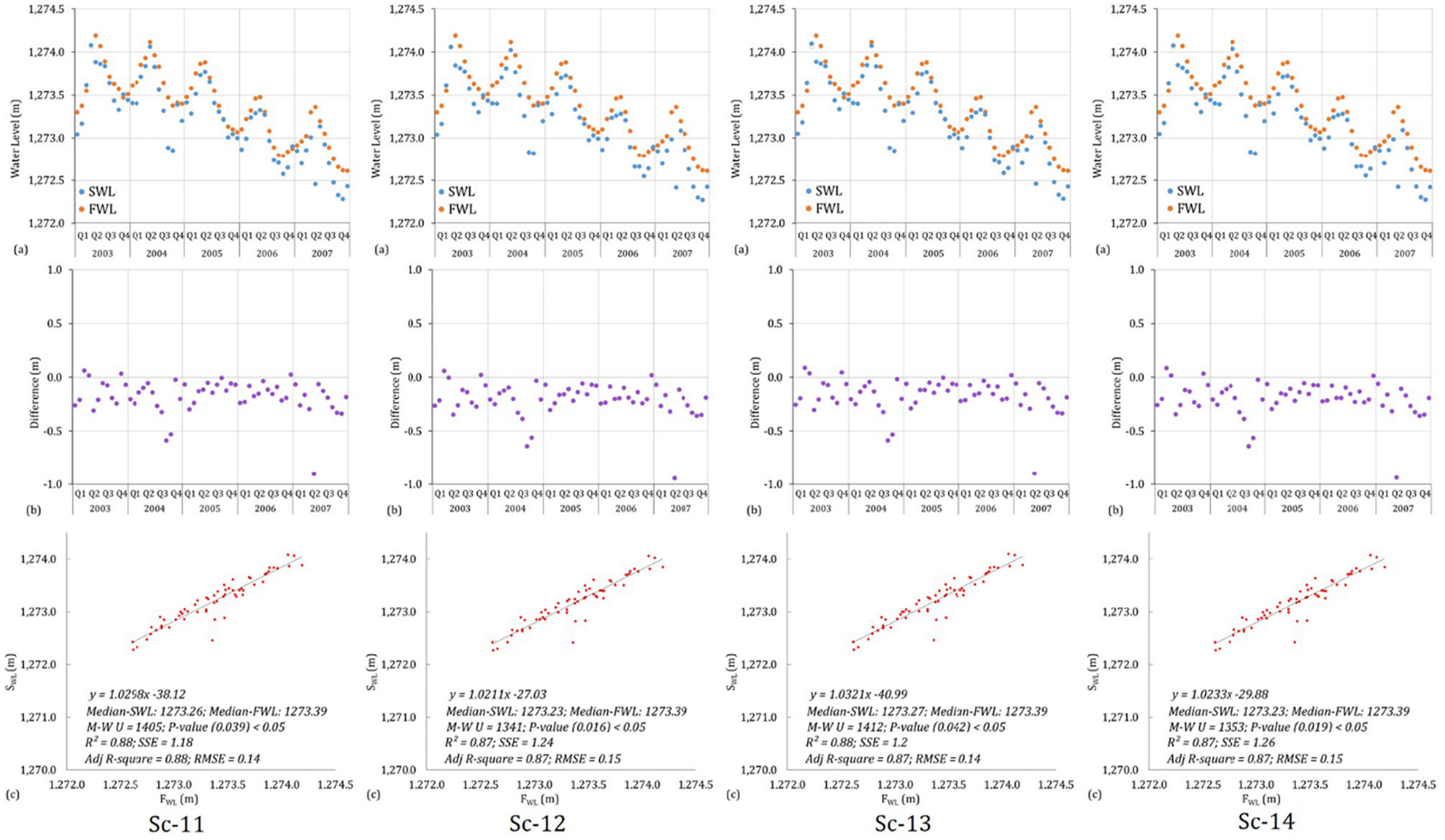

Fig. 5. Combination of multiple data sources based on HW_{WL} as initial WL of the simulation to simulate WL in Lake Urmia for Sc-11 to Sc-14.

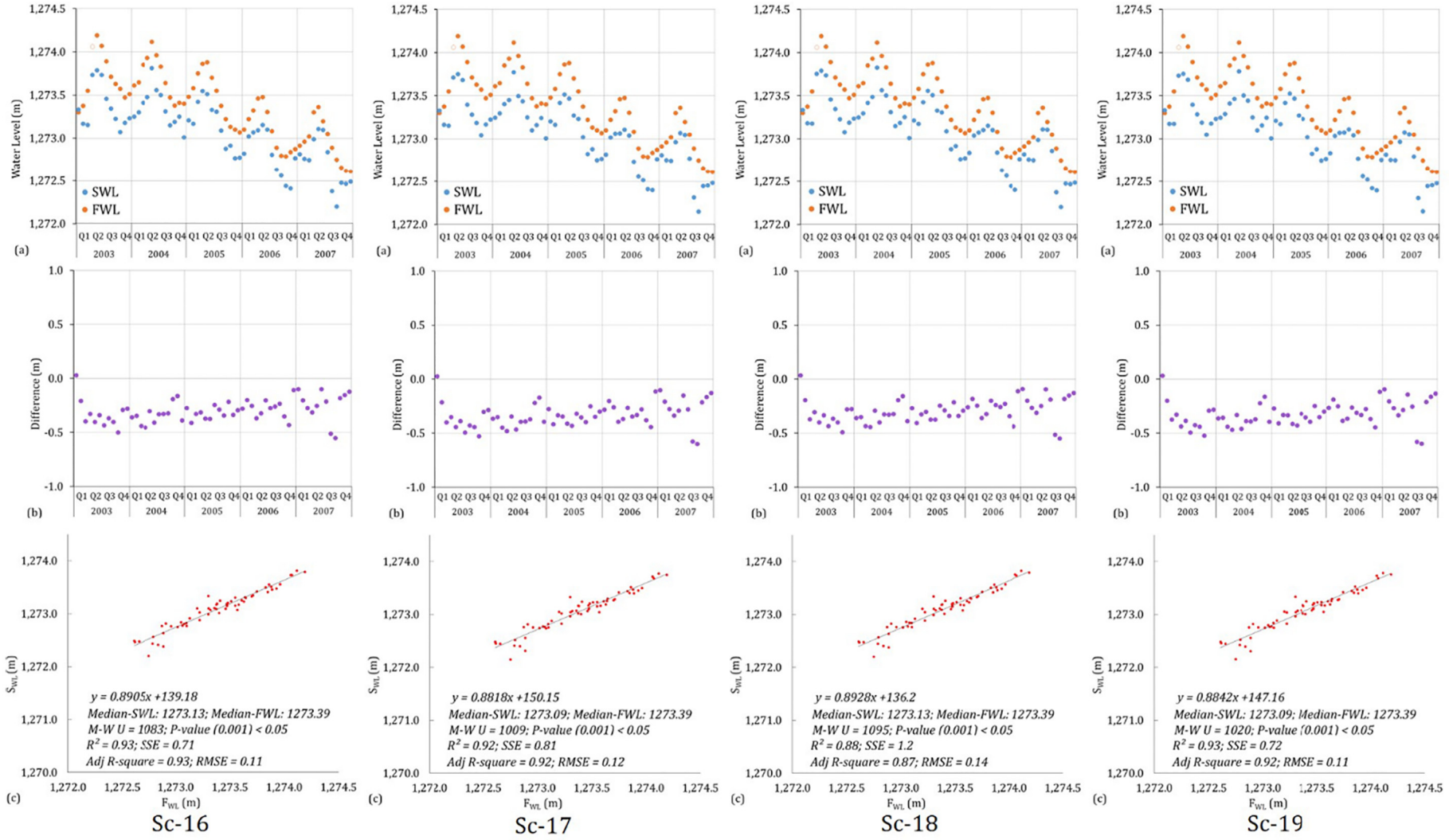

Fig. 6. Combination of different data sources based on DAHITI WL as initial WL of the simulation to simulate WL in Lake Urmia for Sc-16 to Sc-19.

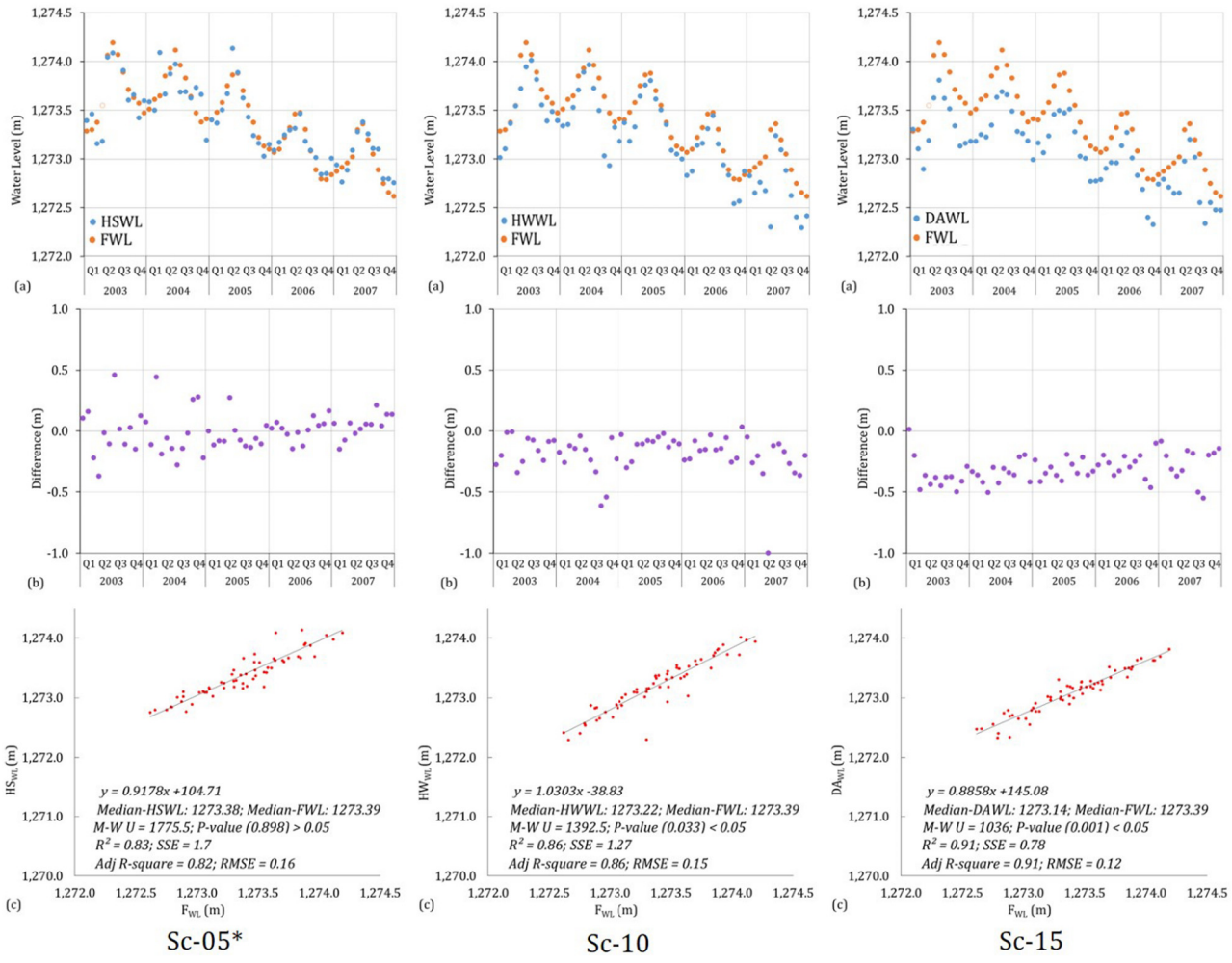

Fig. 7. Temporal variations of Lake Urmia WL: (Sc-5) for Hydrosat and Field WL, (Sc-10) for Hydroweb and Field WL, and (Sc-15) for DAHITI and Field WL. * indicates no significant differences between S_{WL} and F_{WL}.

collected from Lake Urmia. Out of all scenarios, Sc-01 showed the best combination to simulate lake WL by using all hydro-meteorological components from field measurements in the WB simulation algorithm. Without using F_{WL} as the initial WL in the algorithm, we also noticed Sc-08 gave a fair representation of lake WL, although SSE was high (1.3) for this scenario as compared to other significant scenarios. Even without any field data in the algorithm, the proposed scenario combination was capable of predicting WL fluctuations in Lake Urmia (p-value (0.749) > 0.05 in Sc-09).

When different hydro-meteorological components were taken from both satellite and field data, simulated WL showed deviations from the field WL. As expected, this phenomenon was more prominent from Sc-10 to Sc-19 because of the initial WL. The initial conditions are very important for the proposed algorithm. Any error propagates due to the shift of the initial month and WL can significantly influence the whole scenario. Also, factors such as a lack of consideration for outflow from the lake other than evaporation, use of spatially distributed evaporation values to simulate WL, salt, and freshwater differences might play a role in this deviation. Accuracy issues both for field and remotely sensed data sources for different surface water measurements also affected this discrepancy in the output time series of simulated WL.

Surprisingly, except for Hydrosat for other readily available estimated WL time-series, there was a more visible shift in the F_{WL} of Lake Urmia. Although, the estimated WL from DAHITI was already Kalman filtered and the outliers were removed as mentioned by Schwatke et al. (2015). Systematic errors in geophysical corrections, hydrodynamic effects caused by wind and waves might play a role in this shift.

Compared to the estimated WL time series from readily available geodetics sensors, the proposed scenario combination in this study indicated the relative consistency of simulated WL. The RMSE differences varied from 3 cm to 16 cm for all proposed scenarios. The difference was up to 4 cm when field WL was used as initial WL in the scenarios, Sc-01 to Sc-04; but the combination with remotely sensed hydro-meteorological observations led to noisier output time series for other scenarios. We noticed that the higher the effect of multiple component combinations on WL simulation, the higher the RMSE difference was. The same was also applicable for SSE.

The monthly analysis of the WB simulation algorithm is commonly used in many cases (Demlie et al., 2007; Kebede et al., 2006; Muvundja et al., 2014; Troin et al., 2010; Yihdego and Webb, 2012), but our current approach can identify which type of input sources can affect the WL simulation process. Thus, this study emphasizes the possibility of using alternative sources of data for estimating water levels in the lakes, especially when there is a lack of in-situ data to address the managerial issues.

Some environmental changes occur slowly (i.e., groundwater fluxes) and thus the phenomenon may not be addressed in this analysis with the data sources used. For Lake Urmia, we didn't consider groundwater flux as the lake-bed was covered by a thick sediment layer that had been settled for a long period (OWWMP, 2011). Evaluating the contribution of the mid-basin was complicated as it is a function of

irrigation demand in this area and the exact value was not yet measured or reported (Torabi Haghighi et al., 2018). Additionally, the contribution of the ungauged basin and water consumption in this area (irrigation demand) was also ignored from the proposed water balance approach. Furthermore, as the main purpose of this study was to evaluate different scenarios, the items that were ignored affected all scenarios uniformly. Therefore, we propose concentrating more on the proposed algorithm in the future for each different input while simulating WL from raw data sources. Thus, it will be possible to apply the WB simulation approach not only for Lake Urmia but also for other terminal lakes in semi-arid regions. Future studies should focus on including the influence of outflow discharge patterns on lake WL analysis enabling the usability of our method for other types of lake systems.

5. Conclusions

This study integrates multiple driving hydrological components to analyze different scenarios by combining remote sensing and field data with the application of the WB equation in Lake Urmia. We found that considering field data as initial WL can lead us to replicate the fluctuation of Lake Urmia WL in the best way. We observed that Sc-01 (all hydro-meteorological components from field measurements) had the closest simulated WL with the water level collected from Lake Urmia. Remotely sensed rainfall, evaporation from field measurements and initial WL from the Hydrosat platform also showed a better pattern to represent the original lake WL in our analysis. In terms of dynamics, almost all scenarios showed a good pattern, but we found nine out of nineteen scenarios did not vary significantly with the field water level. We noticed no differences between rainfall from the RS source and rainfall from Lake Urmia, which represented a lesser effect of meteorological sources in the WB simulation algorithm. The result also suggests that without any field data in the algorithm, the proposed scenario combination is capable of reproducing WL fluctuation in a lake (Sc-09). The analysis also shows the necessity of using proper data sources when taking action on water regulation and managerial decisions to understand the temporal phenomenon not only for Lake Urmia but also for other terminal lakes in semi-arid regions.

CRediT authorship contribution statement

Joy Bhattacharjee: Conceptualization, Methodology, Formal analysis, Writing – original draft. **Mehedi Rabbil:** Methodology, Formal analysis, Writing – original draft. **Nasim Fazel:** Writing – review & editing. **Hamid Darabi:** Writing – review & editing. **Bahram Choubin:** Writing – review & editing. **Md. Motiur Rahman Khan:** Writing – review & editing. **Hannu Marttila:** Writing – review & editing. **Ali Torabi Haghighi:** Conceptualization, Methodology, Writing – original draft, Investigation, Supervision.

Declaration of competing interest

The authors declare that they have no known competing financial interests or personal relationships that could have appeared to influence the work reported in this paper.

Acknowledgements

We would like to thank all data providers who support us to do the analysis. This work was partially funded by Maj and Tor Nessling Foundation.

Data availability statement

The data that support the findings of this study are available upon reasonable request from the authors (Detailed information about data sources and scenario formation is available in supplemental materials).

Appendix A. Supplementary data

Supplementary data to this article can be found online at https://doi.org/10.1016/j.scitotenv.2021.149034.

References

Akbari, M., Torabi Haghighi, A., Aghayi, M.M., Javadian, M., Tajrishy, M., Kløve, B., 2019. Assimilation of satellite-based data for hydrological mapping of precipitation and direct runoff coefficient for the Lake Urmia Basin in Iran. Water 11. https://doi.org/10.3390/w11081624.

Akbari, M., Baubekova, A., Roozbahani, A., Gafurov, A., Shiklomanov, A., Rasouli, K., Ivkina, N., Kløve, B., Haghighi, A.T., 2020. Vulnerability of the Caspian Sea shoreline to changes in hydrology and climate. Environ. Res. Lett. 15. https://doi.org/10.1088/1748-9326/abaad8.

Anagnostou, E.N., 2004. Overview of overland satellite rainfall estimation for hydrometeorological applications. Surv. Geophys. 25, 511–537. https://doi.org/10.1007/s10712-004-5724-6.

Barhagh, S.E., Zarghami, M., Alizade Govarchin Ghale, Y., Shahbazbegian, M.R., 2021. System dynamics to assess the effectiveness of restoration scenarios for the Urmia Lake: a prey-predator approach for the human-environment uncertain interactions. J. Hydrol. 593, 125891. https://doi.org/10.1016/j.jhydrol.2020.125891.

Buma, W., Lee, S. Il, 2016. Investigating the changes within the Lake Chad Basin using GRACE and LANDSAT imageries. Procedia Eng. https://doi.org/10.1016/j.proeng.2016.07.503.

Crétaux, J.F., Jelinski, W., Calmant, S., Kouraev, A., Vuglinski, V., Bergé-Nguyen, M., Gennero, M.C., Nino, F., Abarca Del Rio, R., Cazenave, A., Maisongrande, P., 2011. SOLS: a lake database to monitor in the near real time water level and storage variations from remote sensing data. Adv. Sp. Res. 47, 1497–1507. https://doi.org/10.1016/j.asr.2011.01.004.

DAHITI, 2021. Home | database for hydrological time series of inland waters (DAHITI) [WWW document]. URL. https://dahiti.dgfi.tum.de/en/. (Accessed 12 March 2021).

Demlie, M., Ayenew, T., Wohnlich, S., 2007. Comprehensive hydrological and hydrogeological study of topographically closed lakes in highland Ethiopia: the case of Hayq and Ardibo. J. Hydrol. 339, 145–158. https://doi.org/10.1016/j.jhydrol.2007.03.012.

Djamali, M., de Beaulieu, J., Shah-hosseini, M., Andrieu-Ponel, V., Ponel, P., Amini, A., Brewer, S., Lahijani, H., Stevens, L., Leroy, S., Akhani, H., 2008. A late Pleistocene long pollen record from Lake Urmia, Nw Iran. Quat. Res. 69, 413–420. https://doi.org/10.1016/j.yqres.2008.03.004.

Fazel, N., Torabi Haghighi, A., Kløve, B., 2017. Analysis of land use and climate change impacts by comparing river flow records for headwaters and lowland reaches. Glob. Planet. Chang. 158, 47–56. https://doi.org/10.1016/J.GLOPLACHA.2017.09.014.

Hofmann, H., Lorke, A., Peeters, F., 2008. Temporal scales of water-level fluctuations in lakes and their ecological implications. Hydrobiologia https://doi.org/10.1007/s10750-008-9474-1.

Huntington, J.L., Hegewisch, K.C., Daudert, B., Morton, C.G., Abatzoglou, J.T., McEvoy, D.J., Erickson, T., 2017. Climate engine: cloud computing and visualization of climate and remote sensing data for advanced natural resource monitoring and process understanding. Bull. Am. Meteorol. Soc. 98, 2397–2409. https://doi.org/10.1175/BAMS-D-15-00324.1.

Hydrosat, 2021. Hydrosat [WWW Document]. URL. http://hydrosat.gis.uni-stuttgart.de/php/index.php. (Accessed 12 March 2021).

Hydroweb, 2021. Hydroweb [WWW Document]. URL. http://hydroweb.theia-land.fr/. (Accessed 12 March 2021).

Jafari, H., Sudegi, A., Bagheri, R., 2019. Contribution of rainfall and agricultural returns to groundwater recharge in arid areas. J. Hydrol. 575, 1230–1238. https://doi.org/10.1016/j.jhydrol.2019.06.029.

Kebede, S., Travi, Y., Alemayehu, T., Marc, V., 2006. Water balance of Lake Tana and its sensitivity to fluctuations in rainfall, Blue Nile basin, Ethiopia. J. Hydrol. 316, 233–247. https://doi.org/10.1016/j.jhydrol.2005.05.011.

Leira, M., Cantonati, M., 2008. Effects of water-level fluctuations on lakes: an annotated bibliography, in: Ecological Effects of Water-Level Fluctuations in Lakes. Springer Netherlands, pp. 171–184. doi:10.1007/978-1-4020-9192-6_16.

Medina, C.E., Gomez-Enri, J., Alonso, J.J., Villares, P., 2008. Water level fluctuations derived from ENVISAT radar altimeter (RA-2) and in-situ measurements in a subtropical waterbody: Lake Izabal (Guatemala). Remote Sens. Environ. https://doi.org/10.1016/j.rse.2008.05.001.

Muvundja, F.A., Wüest, A., Isumbisho, M., Kaningini, M.B., Pasche, N., Rinta, P., Schmid, M., 2014. Modelling lake kivu water level variations over the last seven decades. Limnologica 47, 21–33. https://doi.org/10.1016/j.limno.2014.02.003.

OWWMP, 2011. Iran's comprehensive water resources plan. Groundwater Studies (Lake Urmia Watershed) Report. Iran Ministry of Energy's Office for Water and Wastewater Macro-Planning.

Rezaei Zaman, M., Morid, S., Delavar, M., 2016. Evaluating climate adaptation strategies on agricultural production in the Siminehrud catchment and inflow into Lake Urmia, Iran using SWAT within an OECD framework. Agric. Syst. 147, 98–110. https://doi.org/10.1016/j.agsy.2016.06.001.

Rokni, K., Ahmad, A., Selamat, A., Hazini, S., 2014. Water feature extraction and change detection using multitemporal Landsat imagery. Remote Sens. 6, 4173–4189. https://doi.org/10.3390/rs6054173.

Schmied, H.M., Eisner, S., Fink, G., Flörke, M., Adam, L., Kim, H., Oki, T., Portmann, F.T., Reinecke, R., Riedel, C., Song, Q., Zhang, J., Döll, P., 2016. Variations of global and continental water balance components as impacted by climate forcing uncertainty and

human water use. Hydrol. Earth Syst. Sci. 20, 2877–2898. https://doi.org/10.5194/hess-20-2877-2016.
Schwatke, C., Dettmering, D., Bosch, W., Seitz, F., 2015. DAHITI - an innovative approach for estimating water level time series over inland waters using multi-mission satellite altimetry. Hydrol. Earth Syst. Sci. 19, 4345–4364. https://doi.org/10.5194/hess-19-4345-2015.
Sima, S., Tajrishy, M., 2013. Using satellite data to extract volume-area-elevation relationships for Urmia Lake, Iran. J. Great Lakes Res. 39, 90–99. https://doi.org/10.1016/j.jglr.2012.12.013.
Sima, S., Rosenberg, D.E., Wurtsbaugh, W.A., Null, S.E., Kettenring, K.M., 2021. Managing Lake Urmia, Iran for diverse restoration objectives: moving beyond a uniform target lake level. J. Hydrol. Reg. Stud. 35, 100812. https://doi.org/10.1016/j.ejrh.2021.100812.
Taheri, M., Emadzadeh, M., Gholizadeh, M., Tajrishi, M., Ahmadi, M., Moradi, M., 2018. Investigating the Temporal and Spatial Variations of Water Consumption in Urmia Lake River Basin Considering the Climate and Anthropogenic Effects on the Agriculture in the Basin. https://doi.org/10.1016/j.agwat.2018.11.013.
Torabi Haghighi, A., Kløve, B., 2015. A sensitivity analysis of lake water level response to changes in climate and river regimes. Limnologica 51, 118–130. https://doi.org/10.1016/j.limno.2015.02.001.
Torabi Haghighi, A., Menberu, M.W., Aminnezhad, M., Marttila, H., Kløve, B., 2016. Can lake sensitivity to desiccation be predicted from lake geometry? J. Hydrol. 539, 599–610. https://doi.org/10.1016/j.jhydrol.2016.05.064.
Torabi Haghighi, A., Fazel, N., Akbar Hekmatzadeh, A., Klöve, B., 2018. Analysis of effective environmental flow release strategies for Lake Urmia restoration. Water Resour. Manag. 32, 3595–3609. https://doi.org/10.1007/s11269-018-2008-3.
Troin, M., Vallet-Coulomb, C., Sylvestre, F., Piovano, E., 2010. Hydrological modelling of a closed lake (Laguna Mar Chiquita, Argentina) in the context of 20th century climatic changes. J. Hydrol. 393, 233–244. https://doi.org/10.1016/j.jhydrol.2010.08.019.
Yihdego, Y., Webb, J., 2012. Modelling of seasonal and long-term trends in lake salinity in southwestern Victoria, Australia. J. Environ. Manag. 112, 149–159. https://doi.org/10.1016/j.jenvman.2012.07.002.
Zhang, B., Wu, Y., Zhu, L., Wang, J., Li, J., Chen, D., 2011. Estimation and trend detection of water storage at Nam Co Lake, central Tibetan Plateau. J. Hydrol. https://doi.org/10.1016/j.jhydrol.2011.05.018.